International Journal for Housing Science and Its Applications
Publish August 4, 2025. Volume 46, Issue 3 Pages 9049-9059

https://doi.org/10.70517/ijhsa463177

A study of temporal analysis of EEG signals from patients with Alzheimer's disease using a deep optimization algorithm

Huafang Ding[1], Linlin Dong[1] and Hanxing Gu[1,*]
[1] Department of Gerontology, Qingdao Mental Health Center, Qingdao, Shandong, 266000, China
Corresponding authors: (e-mail: 13306393911@163.com).

Abstract Research on the treatment of Alzheimer's disease based on the analysis of EEG signals can help to cope with the aging of the population. In this paper, the EEG signals of patients were collected as research data by combining channel sampling methods. For the existence of interference artifacts, downsampling method combined with bandpass filter, and independent component analysis are used for signal preprocessing. A time series channel complex network based on deep optimization algorithm is constructed to explore the nonlinear features of EEG signals, and the t-test reveals the pathogenesis of different EEG signal frequency bands. EEG signal acquisition of Alzheimer's disease patients, the characterization of time-level changes in sub-brain regions, and cognitive therapy control-related practices are carried out to verify the validity of the method in this paper. The results showed that the brain regions with more obvious changes in music stimulation were located in the parietal lobe and temporal lobe for the three indexes of arrangement entropy, sample entropy, and Lz complexity in mild to moderate patients ($p<0.05$). The regions with more pronounced changes in severe patients were located only in the temporal lobe. The relative power of the frequency band EEG signals of the patients in the experimental group after treatment were significantly higher than those of the control group and before treatment ($p<0.05$).

Index Terms channel sampling, deep optimization algorithm, time series channel network, EEG signal, Alzheimer's disease

I. Introduction

Alzheimer's disease (AD), also known as dementia, is a primary degenerative brain degenerative disease of the central nervous system, the etiology of which is still unknown. Epidemiologic surveys in China have shown that the prevalence of Alzheimer's disease is about 5%, and AD is the main subtype of dementia in China, with a higher prevalence than vascular dementia and other types of dementia, which has brought a heavy burden to socioeconomic development and health care [1]-[3]. The prevalence of Alzheimer's disease in China has reached 10 million cases, the highest in the world. It is predicted that by 2050, 1 in 85 patients will have Alzheimer's disease, and the number of dementia cases in China will soar to 280 million [4]. Global spending on dementia has increased from $604 billion in 2010 to $818 billion in 2015, a 35.4% increase, and it is expected that spending on dementia-related aspects will increase to $1 trillion in three years [5]. As one of the most common types of dementia in old age, AD is bound to become an important medical and social problem and has received high attention from countries around the world. However, the etiology of AD is still unclear and the pathogenesis is very complex, and experts in the field still believe that it is the result of a combination of factors but is not a normal phenomenon in old age [6]. The disease is often not easy to detect in the early stage, and then the disease will continue to progress slowly, so that the patient's memory, the ability to understand and judge things, sense of direction, common sense, computation and other aspects will be impaired to varying degrees. This is accompanied by changes in sexual behavior, such as a continuous decline in visuospatial function, verbal communication ability, abstract thinking ability, learning and working ability, and self-care ability [7], [8]. When a family member suffers from Alzheimer's disease, it not only affects the patient's own life, but also brings a heavy burden to the whole family.

The diagnosis of Alzheimer's disease has undergone significant changes in the last decade. Traditional diagnosis relies on the assessment of clinical symptoms, such as memory loss, cognitive function decline and other manifestations, combined with neuropsychological tests and imaging to rule out other diseases, but there is a significant lag in this model, and patients are often in the middle to late stages of the disease when they develop typical symptoms, thus missing the optimal window for intervention [9], [10]. In recent years, EEG has been widely used in neuroscience research, such as the study of brain cognitive function, emotion regulation, and state of consciousness. By analyzing EEG under different tasks, EEG signals can reflect the cognitive activity changes of the brain in both time and space dimensions, which directly records the brain neural activity, and EEG signals are

multidimensional signals, and the spatial distribution of multi-electrodes can explore the characteristic changes of different brain regions [11]. It can reveal the relationship between brain activity and behavior, and deeply understand the functional mechanism of the brain, and it shows a big potential in the diagnosis and treatment of AD due to its high efficiency temporal resolution, ability to capture transient EEG activity, and low cost, non-invasive, and convenient features [12]-[14].

With the gradual increase in the number of AD patients, researchers have proposed a variety of methods to more accurately analyze the temporal characteristics of their EEG signals. Literature [15] based on wavelet coherence, quantile map, fractal dimension, quadratic entropy, wavelet energy, and visibility map for the temporal analysis of EEG signals in AD showed that the first two analysis methods were stable and effective in identifying whether an elderly individual suffered from AD. Literature [16] applied two methods, multi-scale entropy analysis and multiple fractal analysis, to analyze the AD EEG signal time series separately, which improved the classification accuracy of AD. With the development of algorithmic models, literature [17] used Fourier transform and wavelet transform to capture the time-frequency features of EEG signals, combined with tree-supervised model to classify them, and the classification accuracy of AD was as high as 79%-83%, in which wavelet transform was better than Fourier transform. Literature [18] used the K-nearest neighbor algorithm to classify the frequency and time-frequency features of AD EEG signals to determine whether the experimenter had AD, and the method had a 99% correct rate in short dynamic (eye-opening) behavior. In deep learning algorithms, literature [19] detects AD by generating AD features and predicting AD prevalence based on spatiotemporal AD EEG signals under a convolutional neural network (CNN) model with two convolutional and softmax layers with fewer network parameters. Literature [20] extracted AD spatio-temporal features by recurrent neural network and multi-scale expansion CNN, combined with enhanced wild goose lemur optimization algorithm to determine the feature weights, and finally used the optimizer's attentional long and short-term memory for AD detection. In terms of optimization algorithms, literature [21] combined principal component analysis, particle swarm optimization algorithm, and gated recurrent unit to analyze AD EEG signal temporal features, and the classification accuracy of diagnosing AD was as high as 93.51%. Although the accuracy of deep learning and optimization algorithms in the timing analysis of AD EEG signals is more than 90%, the generalization of these analysis methods for data collected by different EEG signal devices is not high, and lack of interpretability and high requirements for computational storage space, which leads to a reduction in the effect of timing analysis in depth. In contrast, deep optimization algorithms, which embed optimization algorithms in deep learning to strengthen the model performance with its minimization loss function, excel in global feature search and abstract feature analysis, providing a superior analysis method for EEG signal timing analysis [22].

In this paper, EEG signals and related data information of patients are collected by EEG instruments to establish a research dataset. Using a combination of filter techniques and signal decomposition methods, the EEG signals are preprocessed with interference artifacts to obtain clean EEG data. The nonlinear characteristic parameters such as Petrosian fractal dimension, Hurst coefficient, Lempel-Ziv complexity, etc. of the EEG signals are calculated to analyze the correlation between the EEG signals and the time series, and to explore the causes of the onset of the disease. Patient data collected from hospitals were used as the basis of the study to analyze whether the EEG channel acquisition was effective. The EEG signals were divided into brain regions to study the nonlinear characteristic parameters. According to the different degrees of disease, analyze the differences in stimulation response of corresponding brain regions. Combine the mining results with the treatment to verify the practical value of the method in this paper.

II. Technical support related to EEG signal timing analysis

This chapter analyzes the objects and methods involved in the study. It details how a complex network model of time series channels, based on deep optimization algorithms, can be applied to the analysis of EEG signals in patients with Alzheimer's disease.

II. A. Study population and methodology

II. A. 1) Subject of the study

We collected all patients with a diagnosis of mild cognitive impairment (MCI) and Alzheimer's disease (AD) who attended a university hospital from February 2019 to September 2024 and completed resting-state EEG examinations. The subjects were of Han Chinese ethnicity, and MCI patients were enrolled as those diagnosed with “MCI meeting the core clinical diagnostic criteria” according to the criteria of the Alzheimer's Disease Association (NIA-AA). Patients with AD were enrolled as those diagnosed with “probable AD” according to the NIA-AA criteria. The diagnosis and classification of epileptic seizures were based on the criteria proposed by the International League Against Epilepsy (ILAE). All diagnoses were made by 2 experienced neurologists. Patients with any of the following characteristics were excluded:

(1) History of distant epileptic seizures (defined as epileptic seizures occurring 4 years before the onset of cognitive impairment);

(2) Patients with previous seizures caused by cortical lesions, acute metabolic disorders, or subdural hematomas;

(3) Other causes of dementia: such as dementia caused by Lewy body dementia, frontotemporal lobe dementia, Parkinson's disease dementia and other degenerative dementias, central nervous system infections (e.g., AIDS, syphilis, etc.), Creutzfeldt-Jakob disease, autoimmune encephalopathies, traumatic brain injuries, intracranial tumors, Huntington's disease of chorea, dementia caused by drugs, alcohol, and CO intoxication, and other causes of dementia caused by severe somatic illnesses (e.g., hepatic encephalopathy, pulmonary encephalopathy, etc.). Dementia caused by other reasons such as severe physical diseases (e.g. hepatic encephalopathy, pulmonary encephalopathy)

(4) Those who did not agree to sign the informed consent form.

The above exclusion criteria were referenced from previous exclusion criteria in similar studies investigating epileptic seizures in patients with dementia. All participants signed an informed consent form before inclusion in the study, on the premise of informing the patients themselves and their families in detail about the contents of the study. Patients were queried for epileptic seizures through the electronic medical record system and telephonically asked if they and their caregivers had epileptic seizures. A total of 200 patients with MCI and 300 patients with AD were finally included in this study. The study followed the basic principles of the Declaration of Helsinki, an international code of medical ethics, and was reviewed by the hospital ethics committee.

Clinical information about each patient was collected, including demographic data such as gender, year of birth, and education level, general clinical data including personal and family history, cardiovascular risk factors (hypertension, dyslipidemia, diabetes mellitus), magnetic resonance results of the head, medications (anticholinergic, anti-NMDA, and psychotropic), epileptic seizures with or without epileptic episodes, duration of epileptic episodes, type of epileptic episodes, medication, the As well as a neuropsychological assessment of all MCI and AD patients, which consisted mainly of the clinically widely used Brief Mental Status Examination Scale (MMSE), Montreal Cognitive Assessment Scale (MoCA), and Clinical Dementia Rating Scale (CDR). We collected and evaluated resting-state EEG data for all MCI and AD patients.

II. A. 2) EEG acquisition and analysis methods

A Nicolet EEG (V32-20020130) instrument according to the 10-20 International System using standard 19-channel leads (Fp1, Fp2, F3, Fz, F4, F7, F8, T3, T4, T5, T6, C3, Cz, C4, P3, Pz, P4, O1, O2) was used with a sampling rate of 205 Hz under resting conditions with eyes closed to The participants' EEG signals were recorded for 15 minutes. Figure 1 shows the locations of the 19 electrode placements for the International 10-20 system. Participants were asked to remain awake throughout the monitoring.

All EEG monitoring was done by the same experienced EEG practitioner who was uncertain about the subject's diagnosis. All EEG data were diagnostically graded by 2 experienced EEG physicians who were unclear about the diagnosis according to the diagnostic grading criteria, which grades background abnormalities only, and can be categorized as normal EEG, borderline state EEG, mildly abnormal EEG, moderately abnormal EEG, and severely abnormal EEG; paroxysmal abnormalities (epileptiform discharges) are described separately, and epileptiform discharges primarily Epileptiform discharges include spikes or sharp waves.

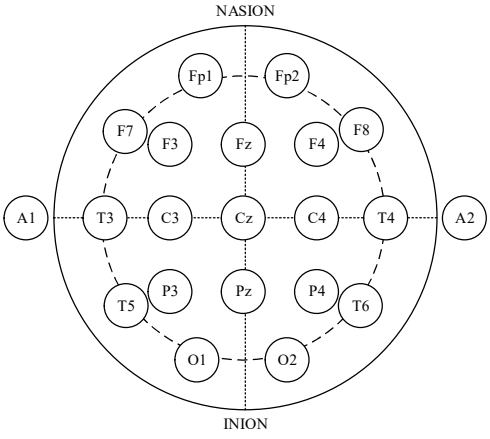

Figure 1: Positions where 19 electrodes of the International 10-20 system are placed

II. B.EEG signal preprocessing

In the process of EEG signal acquisition, subjects will be subjected to external interference and artifacts, which can be mainly categorized into environmental artifacts, electromagnetic artifacts and biological artifacts. Environmental artifacts mainly include 45 Hz IF interference from AC power, signal jumps caused by building vibration, and geomagnetic noise from nearby elevators, cell phones, and geomagnetic fields. Electromagnetic artifacts include electromagnetic interference from stimulus presentation, continuous oscillations of the head position indicator coil at a specific frequency, and random high amplitude fluctuations due to sensor malfunction. Biological artifacts contain periodic signal disturbances caused by cardiac activity, transient deflections of signals induced by eye movements and blinking, and EMG artifacts caused by muscle activity during swallowing jerks. In the experiments, the most significant effects on EEG signal analysis were IF interference, cardiac artifacts, and EMG artifacts.

Since the EEG signal acquisition process is inevitably interfered by external factors to produce artifacts, the raw EEG signal data acquired need to be preprocessed before using the EEG signal for model training. Commonly used methods in the pre-processing stage are re-referencing, filter techniques, and signal decomposition methods. Re-referencing means using the average potential of the left mastoid as a reference to solve the problem of asymmetry between left and right brain activities, or using the average potential of all electrodes as a reference to solve the problem of displaying EEG activities at some electrodes. The filter technique is based on the fact that the effective components of the EEG signal are mainly located in the 1-40 Hz frequency band, and a better de-artifactualization effect can be achieved by filtering the signal to a certain range using a band-pass filter. Signal decomposition methods include methods such as independent component analysis (ICA) and signal space projection (SSP).ICA is a technique for estimating independent source signals from a set of recordings in which the individual source signals are mixed in unknown proportions, and is commonly used in the problem of blind source separation.The SSP technique is a technique that removes the noise by projecting the EEG signal into a low-dimensional space.The average pattern of the signal is computed to select the subspaces and to construct a subspace orthogonal to the direction of the noise, and the noise is removed by projecting the signal into the subspace.

In the experiments of this paper, the dataset used to collect signals with channel Fz as the reference electrode, which can effectively represent the EEG activity at each electrode, so there is no need to re-reference the EEG signals. In this paper, a downsampling method is used to remove the high frequency components, and then a band-pass filter is used to filter the EEG signals obtained from 1 Hz to 40 Hz. However, there are still artifacts in the low frequency band in the signal recording, in order to get clean EEG data, this paper also uses independent component analysis for processing. The specific steps of independent component analysis are as follows: receive the observed signals, standardization of the mean value of the data recommendations, principal component analysis processing of the observed data matrix, and then align the whitening process, through the calculation of each independent component, and finally through the independent component reconstruction to eliminate the components that are close to the frequency band of the EEG signals, with the following specific formulas:

where $X \in R^{m\times n}$ is the data matrix, m is the number of measured variables, n is the total number of samples, $A \in R^{m\times n}$ is the mixing matrix, $s \in R^{n\times n}$ is the matrix composed of the independent components, $E \in R^{m\times n}$ is the residual matrix.

II. C.Time series channel complex network construction

II. C. 1) Nonlinear characteristics

1) Petrosian Fractal Dimension (PFD)

Petrosian Fractal Dimension (PFD) Fractal dimension is a chaotic method of calculating the complexity of a signal.PFD helps in calculating the fractal dimension quickly.PFD performs this process by converting the signal into a binary sequence. It can be estimated by the following expression:

$$PFD = \frac{\log_{10} k}{\log_{10} k + \log_{10}\left(\frac{k}{k+0.4N_{\delta}}\right)} \tag{1}$$

where k is the number of signal sampling points and N_{δ} is the number of signal variations.

2) Hurst Exponent (HE)

The Hurst exponent is used to measure the long-range dependence within the signal, ranging from 0-1. The Hurst coefficient is used in EEG time-series analysis to present the non-smooth/antistatic EGG states observed during sleep. HE was defined:

$$HE = \frac{\log\left(\frac{R}{S}\right)}{\log(T)} \tag{2}$$

Here, T is the data sampling rate and R/S is the value of the rescaling range. In Hurst exponent, H=0.55 denotes a signal with the property of random wandering or Brownian motion. H<0.55 the length of time series has a negative correlation with memory, while the value H>0.55 indicates that the time series is characterized by long-term memory.

3) Lempel-Ziv complexity (Lz)

The Lempel-Ziv complexity algorithm is a method to characterize the rate of emergence of new patterns in a time series, which is highly robust to interference and noise, and has a great advantage for characterizing highly unstable brainwaves, and can reveal the correlation patterns of the human brain to a certain extent.The steps for calculating the Lz complexity are:

(1) Calculate the mean value of the EEG time series, and divide the time series into two parts according to the size of the EEG time series in relation to the mean value, and if you want to divide the already divided part of the EEG time series again, you can use the same method to divide it.

(2) Compare the first value of the sequence with the average value, if it is greater than the average value it is 1, if it is not greater than the average value it is 0; the formula is:

$$s_i = \begin{cases} 0 & x_i < \tau \\ 1 & x_i \geq \tau \end{cases} \text{among } i = 1 \tag{3}$$

Starting from the second value of the EEG time series, the result of binarization is related to the previous point of the comparison and is assigned a value of 1 if it increases to another region, 0 if it decreases to another region, and stays the same value as the previous point if there is no change from the previous value with the formula:

$$s_i = \begin{cases} 0 & x_i < x_{i-1} \text{And they are no longer in the same area} \\ 1 & x_i \geq x_{i-1} \text{And they are no longer in the same area} \\ s_{i-1} & \text{other} \end{cases} \tag{4}$$

Using Lz complexity for feature extraction of EEG signal can retain more detailed information of EEG time series and can improve the accuracy of feature extraction. The normalized Lz complexity formula is:

$$C = \frac{c(n)\log_i n}{n} \tag{5}$$

where $c(n)$ is the Lz complexity of the EEG time series, and n is the length of the EEG time series. i is the number of coarse-grained segments of the time series. Figure 2 shows the specific process.

II. C. 2) Time series network property analysis

In this section, we mainly want to analyze the characteristics between normal people and patients' attributes by studying the attributes of the constructed networks, and find out their differential attributes to discover the differences of their constructed networks.

According to the existing research in the subject group, it is known that normal people and patients have significant differences in the α band and θ band, and the differential channels are different in different bands at different stages. In this thesis, by constructing networks for these channels and analyzing the differences of their networks constructed on time series through network properties, we provide a basis for further revealing their pathogenesis.

By finding the attributes such as average clustering coefficient, global efficiency, average local efficiency, module value and average path length of each network of each channel, the t-test is performed on the requested attributes. t-test is a widely used test for determining whether there is a statistically significant difference between two sets of averages. t-test formula is as follows, the upper half of the formula is the mean of the two samples or the difference between the means, and the lower half of the formula is the distribution of the variable or the distribution of the data. t-test formula is:

$$t = \frac{|\mu_0 - \mu_l|}{\sqrt{\left(\frac{1}{n_0} + \frac{1}{n_l}\right)\frac{(n_0 - l)\sigma_0^2 - (n_l - l)\sigma_l^2}{n_0 + n_l - 2}}} \tag{6}$$

where μ_i, σ_i^2 and n_i denote the mean, variance, and sample size of the i th sample class, respectively.

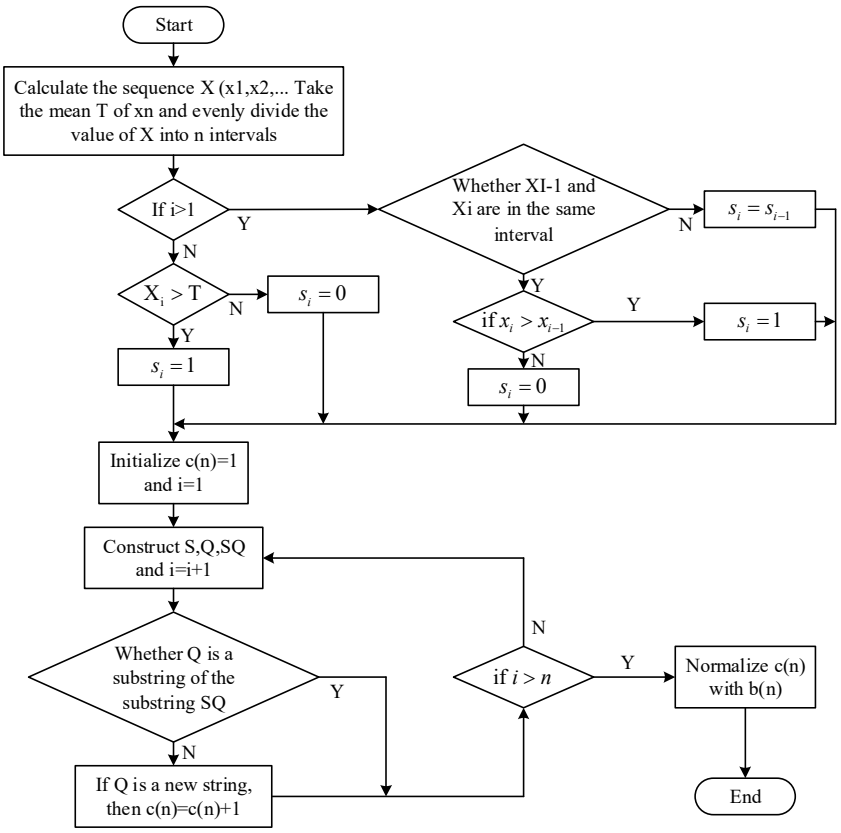

Figure 2: The calculation process of Lempel-Ziv complexity

III. Deep optimization-based timing analysis practice

This chapter verifies the application value of the method of this paper through specific EEG signal analysis practice and cognitive therapy practice based on EEG signal analysis.

III. A. Experimental data

Table 1 shows the information of the data related to the top 15 patients for EEG acquisition. The constructed dataset is derived from the EEG acquisition of hospital patients, which contains prolonged multichannel EEG recordings of 500 patients with a sampling frequency of 250 Hz. EEG recordings of all patients were acquired through 19 channels: Fp1, Fp2, F3, Fz, F4, F7, F8, T3, T4, T5, T6, C3, Cz, C4, P3, Pz, P4, O1, O2. As can be seen in Table 1, the patients were all over 50 and under 70 years of age. The number of seizures ranged from 4-20, with a large variation in the number of seizures in different patients. Seizure durations ranged from [154,1990]s and the variation in seizure durations was also high in different patients. Non-epileptic durations ranged from 19.73-143.95h. Overall, the experimental data contained EEG information from several different patients, meeting the diversity requirements of the experiment.

III. B. EEG channel analysis

In order to verify the validity of the EEG signal acquisition in this paper and reduce the influence on the subsequent experimental analysis, the coherence of the different channels of EEG signal features (MST-CPC) and EMG features was analyzed by comparing which channel has a higher degree of correlation with the EMG features, so as to determine that the EEG signals are valid.The dimension of the MST-CPC features is 188×130, and that of the EMG features is 6×30, and since the number of the number of sampling points are 130 and 30 respectively, the data are divided into 3 segments for coherence analysis. The EEG Fz channel was visualized as an example.

Figure 3 shows the coherence between the MST-CPC features of the EEG Fz channel and the EMG features of 15 patients. The 3 subplots in Figure 3(a) show the coherence of different 3 segments of feature 1 of the EEG Fz channel MST-CPC features with EMG, respectively. The 3 small plots in Fig. 3(b) show the coherence of different 3 segments in feature 2 of the EEG Fz channel MST-CPC feature with EMG, respectively. As can be seen from Fig.

3, the coherence of MST-CPC features 1 and 2 of the EEG Fz channel with EMG features remains highly consistent, with the coherence coefficient error not exceeding 0.1, and the trend of the coherence coefficient change of each segment of feature 1 and the corresponding segment of feature 2 with EMG features is the same. From this, it is judged that the EEG signals acquired using the channel in this paper have usability.

Table 1: Data information (Top 15)

Patient	Gender	Age	Number of channels	Frequency of epileptic seizures	Duration of epilepsy /s	Non-epileptic duration /h
1	F	61	19	8	441	40.45
2	M	59	19	7	173	35.23
3	F	62	19	10	404	38.87
4	M	55	19	5	376	143.95
5	F	63	19	7	555	38.84
6	F	61	19	12	154	62.97
7	F	58	19	4	327	62.94
8	M	57	19	7	918	19.73
9	F	66	19	8	275	67.77
10	M	53	19	6	444	49.91
11	F	67	19	15	803	34.58
12	F	68	19	9	1477	23.25
13	F	65	19	5	532	32.86
14	F	63	19	7	167	25.97
15	M	57	19	20	1990	39.44

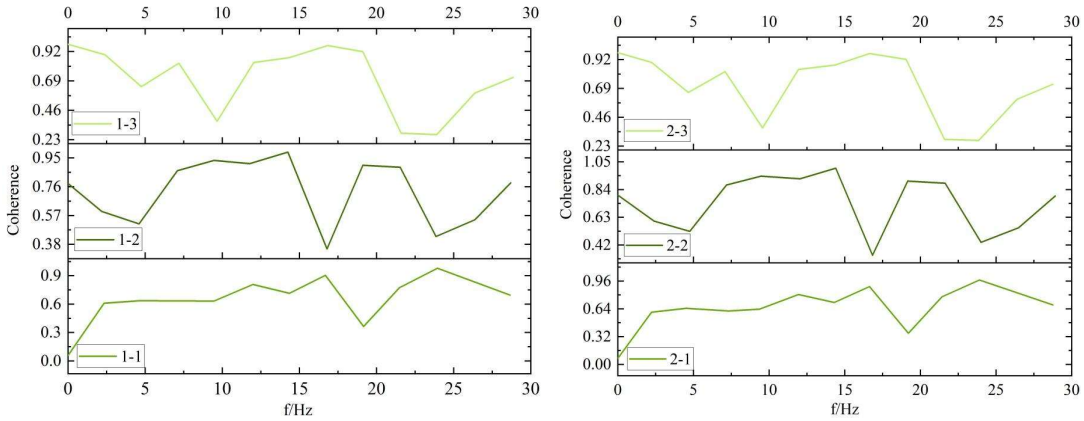

(a) Coherence of 3 different segments in Feature 1 with electromyography

(b) Coherence of 3 different segments in Feature 2 with electromyography

Figure 3: Coherence between MST-CPC and electromyographic characteristics

III. C. Sub-brain area time level results based on nonlinear feature parameters

III. C. 1) Results of changes in time-level alignment entropy in sub-brain regions

Using the complex network of time series channels constructed in this paper, the results at the time level of sub-brain regions are studied from the perspective of nonlinear characteristics. Figure 4 shows the results of the change in alignment entropy at the time level of sub-brain regions. Compared to pre-stimulation, the regions where more significant changes in the alignment entropy values of mild to moderate patients were found in music stimulation were located in the parietal and temporal lobes ($p<0.05$).

1) Manifested as significantly higher entropy values in the parietal lobe during stimulation compared to pre-stimulation ($p=0.0122$), and also significantly higher in the parietal lobe post-stimulation compared to pre-stimulation ($p=0.00902$). Previous studies have shown that Alzheimer's cognitive level is related to parietal lobe activity and that entropy values and complexity gradually increase as cognitive ability improves. Therefore, changes in parietal lobe arrangement entropy over time can be interpreted as cognitive improvement in mild-to-moderate patients.

2) The entropy value of the temporal lobe in mild-to-moderate AD decreased significantly in the stimulus compared to the pre-stimulus (p=0.00145). Since emotional dysregulation is associated with abnormal brain activity in the right middle temporal gyrus, the temporal lobe may have a function in regulating emotions, and therefore, the change in temporal lobe arrangement entropy over time can be interpreted as a relief of emotions during musical stimulation in mild-moderate patients.

The alignment entropy values in the severe group showed a significant difference only in the temporal lobe during musical stimulation (p<0.05), as indicated by a lower entropy value in the temporal lobe stimulation compared to the pre-stimulation (p=0.001623). This change is partially similar to the above trend of entropy change in temporal lobe arrangement in mild to moderate patients, which can be interpreted as emotional regulation and anxiety relief during music stimulation in severe patients.

Compared to pre-stimulation, the arrangement entropy of the frontal, temporal and parietal lobes in the healthy control group were all significantly different during musical stimulation. The difference between the healthy control group and the mild-moderate patients is that in addition to the parietal lobe, the EEG arrangement entropy of the temporal lobe changed significantly during music stimulation, and the EEG arrangement entropy of the frontal lobe of the healthy control group also changed significantly, which is due to the fact that the frontal lobe is responsible for higher cognitive functions, and the brain responses of the healthy control group under music stimulation possessed high-level cognitive responses in addition to the simple cognitive responses and emotional responses.

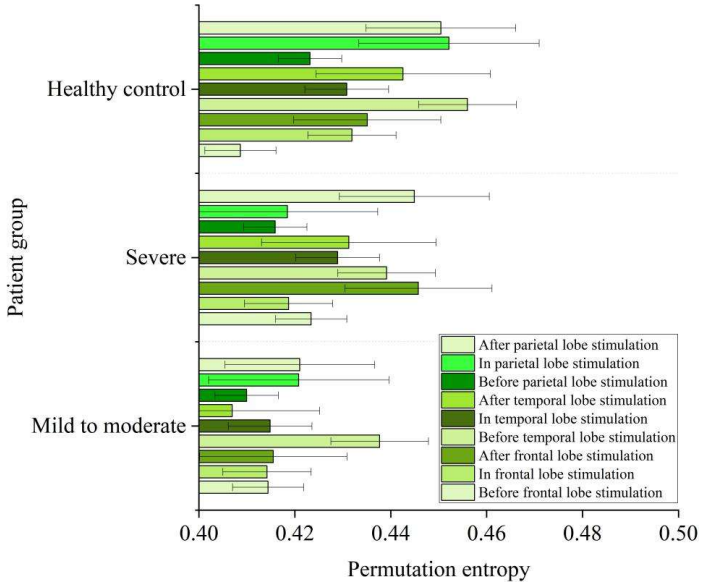

Figure 4: Arrange the entropy changes at the temporal level by brain regions

III. C. 2) Results of changes in sample entropy at the time level of sub-brain regions

The sample entropy and LZ complexity are similar to the arrangement entropy law. Figure 5 shows the results of changes in sample entropy at the temporal level in sub-brain regions. Significant changes in sample entropy values were found in the parietal and temporal lobes of the mild-moderate patient group in musical stimulation compared to pre-stimulation (p<0.05). The results showed that the entropy values of the parietal lobe were significantly higher during and after the stimulation compared to the pre-stimulation (p=0.00008 for pre- and mid-stimulation. p=0.02103 for pre- and post-stimulation). Entropy values of the temporal lobe were significantly decreased both during and after stimulation compared to pre-stimulation (pre-stimulation and stimulation, p=0.0019. pre-stimulation and post-stimulation, p=0.00064). The only region that showed a significant difference in sample entropy values between music stimulation and post-stimulation for the severe group compared to pre-stimulation was located in the temporal lobe (p<0.05). Their relative ability profile was consistent with that of the moderate group. The relative energy of the temporal lobe was lower in both during and after stimulation compared to pre-stimulation (pre and during stimulation, p=0.0019. pre and post stimulation, p=0.00064). Significant changes in entropy entropy of healthy pairs of samples during and after musical stimulation compared to pre-stimulation were located in three brain regions (frontal, temporal, and parietal lobes).

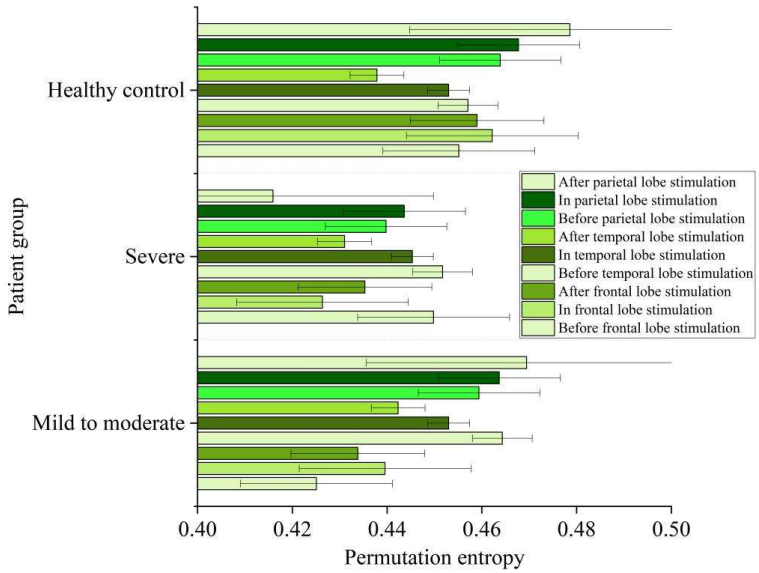

Figure 5: Changes in sample entropy at the temporal level by brain regions

III. C. 3) Results of changes in LZ complexity at the time level of sub-brain regions

Figure 6 shows the results of changes in LZ complexity at the temporal level in sub-brain regions. The LZ complexity values of the parietal and temporal lobes in the mild-moderate patient group showed significant changes during musical stimulation ($p<0.05$), as evidenced by significantly higher entropy values of the parietal lobes during and after stimulation compared to pre-stimulation (pre-stimulation and stimulation, $p=0.00007$. pre-stimulation and post-stimulation, $p=0.003$). The only region that showed a significant difference in LZ complexity values in the heavy group during and after musical stimulation compared to pre-stimulation was located in the temporal lobe ($p<0.05$), as evidenced only by a higher relative energy during and after stimulation compared to pre-stimulation (pre-stimulation and stimulation, $p=0.00122$. pre-stimulation and post-stimulation, $p=0.00043$). Significant changes in LZ complexity values in the frontal, temporal and parietal lobes of healthy controls occurred during and after musical stimulation compared to pre-stimulation in three brain regions (frontal, temporal and parietal lobes).

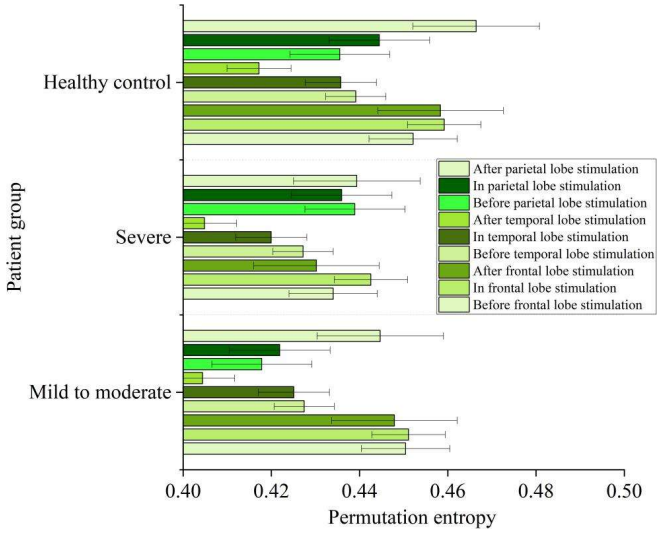

Figure 6: Changes of LZ complexity at the temporal level by brain regions

III. D. Comparison of EEG signals before and after treatment

The 500 patients included in the dataset were equally divided into two groups for a controlled experiment. The experimental group was treated with continuous cognitive therapy using a time series channel complex network based on a deep optimization algorithm, and the control group was treated with traditional cognitive therapy methods. EEG characterization was performed at the time of enrollment and after 4 months of continuous treatment in both

groups. Digital EEG equipment was selected for EEG characterization, and the ratio of EEG signal power changes in different frequency bands was determined. The collected data were statistically analyzed by SPSS 18.0 software, the count data were tested by x2 test, and all the measurement data were expressed by ($\bar{x}$ ±s), and the t-test was used for the comparison of the groups, and the difference was considered to be statistically significant when P < 0.05.

Table 2 shows the results of the comparison of the relative power ratios of different frequency bands of the EEG signals of the two groups of patients before and after treatment ($\bar{x}$ ±s). The difference in the relative power of EEG signals of α 1, α 2, β 1 and β 2 frequency bands before the treatment of the two groups of patients was not statistically significant (P > 0.05), and the relative power of EEG signals of α 1, α 2, β 1 and β 2 frequency bands of the patients of the experimental group after the treatment was significantly higher than that of the control group with the pre-treatment (P < 0.05). According to the comparison results of EEG signals before and after treatment, it can be found that the use of the time series channel complex network based on the depth optimization algorithm in this paper to analyze the signals of various brain regions of the patients, and to provide targeted cognitive therapy based on the results obtained can significantly enhance the activity of EEG signals of the Alzheimer's disease patients and improve the cognitive level.

Table 2: Comparison results of 2 groups of patients before and after treatment

Group	α_1				α_2			
	Before treatment	After treatment	T-value	P-value	Before treatment	After treatment	T-value	P-value
Experimental group	1.156±0.298	1.428±0.216	4.663	0.001	1.117±0.317	1.411±0.146	5.345	0.000
Control group	1.161±0.255	1.172±0.145	0.236	0.816	1.154±0.293	1.172±0.317	0.267	0.795
T-value	0.082	6.124	-	-	0.540	4.345	-	-
P-value	0.937	0.001	-	-	0.593	0.001	-	-
Group	β_1				β_2			
	Before treatment	After treatment	T-value	P-value	Before treatment	After treatment	T-value	P-value
Experimental group	0.879±0.214	1.261±0.326	6.125	0.000	0.668±0.424	1.057±0.243	5.167	0.000
Control group	0.868±0.246	0.854 ±0.273	0.243	0.812	0.672±0.206	0.637±0.107	0.944	0.352
T-value	0.210	6.037	-	-	0.055	10.681	-	-
P-value	0.834	0.001	-	-	0.956	0.000	-	-

IV. Conclusion

This paper applies a time series channel network based on a deep optimization algorithm to analyze the specific changes in the EEG signals of patients with Alzheimer's disease to achieve targeted cognitive therapy. The brain regions of patients with mild to moderate severity were able to respond to musical stimuli. Significant changes in EEG signals were located in the parietal and temporal lobes in mild to moderate patients (p<0.05), and only in the temporal lobe in severe patients (p<0.05). Based on the results of sub-brain area time series analysis for control experiments, the relative power of frequency band EEG signals of patients in the experimental group was significantly higher than that of the control group (p<0.05). At the same time, the relative power of frequency band EEG signal in the experimental group after treatment was also significantly higher than that before treatment (p<0.05). The EEG activity and cognitive ability of Alzheimer's disease patients can be enhanced using the method in this paper. In the future, real-time monitoring technology can be further introduced into the time series channel network based on deep optimization algorithm to improve the timeliness of EEG signal analysis.

References

[1] Kanglan, L., Shouchao, W., Zhou, L., Li, H., Jiajing, L. I. N., Shiting, T. A. N., ... & Guifeng, T. U. (2018). The prevalence of Alzheimer's disease in China: a systematic review and meta-analysis. Iranian journal of public health, 47(11), 1615.

[2] Bo, Z., Wan, Y., Meng, S. S., Lin, T., Kuang, W., Jiang, L., & Qiu, P. (2019). The temporal trend and distribution characteristics in mortality of Alzheimer's disease and other forms of dementia in China: Based on the National Mortality Surveillance System (NMS) from 2009 to 2015. PloS one, 14(1), e0210621.

[3] Jia, J., Wei, C., Chen, S., Li, F., Tang, Y. I., Qin, W., ... & Gauthier, S. (2018). The cost of Alzheimer's disease in China and re-estimation of costs worldwide. Alzheimer's & Dementia, 14(4), 483-491.

[4] Clay, E., Zhou, J., Yi, Z. M., Zhai, S., & Toumi, M. (2019). Economic burden for Alzheimer's disease in China from 2010 to 2050: a modelling study. Journal of market access & health policy, 7(1), 1667195.
[5] Li, X., Feng, X., Sun, X., Hou, N., Han, F., & Liu, Y. (2022). Global, regional, and national burden of Alzheimer's disease and other dementias, 1990–2019. Frontiers in aging neuroscience, 14, 937486.
[6] Adams, J. D. (2021). Probable causes of Alzheimer's disease. Sci, 3(1), 16.
[7] Kozlov, S., Afonin, A., Evsyukov, I., & Bondarenko, A. (2017). Alzheimer's disease: as it was in the beginning. Reviews in the Neurosciences, 28(8), 825-843.
[8] Clifford, K., Moreno, M., & Kloske, C. M. (2024). Navigating late-stage dementia: a perspective from the Alzheimer's Association. Alzheimer's & Dementia: Diagnosis, Assessment & Disease Monitoring, 16(1), e12530.
[9] Wolinsky, D., Drake, K., & Bostwick, J. (2018). Diagnosis and management of neuropsychiatric symptoms in Alzheimer's disease. Current psychiatry reports, 20, 1-13.
[10] Beata, B. K., Wojciech, J., Johannes, K., Piotr, L., & Barbara, M. (2023). Alzheimer's disease—Biochemical and psychological background for diagnosis and treatment. International journal of molecular sciences, 24(2), 1059.
[11] Ismail, L. E., & Karwowski, W. (2020). Applications of EEG indices for the quantification of human cognitive performance: A systematic review and bibliometric analysis. Plos one, 15(12), e0242857.
[12] Erickson, M. A., Kappenman, E. S., & Luck, S. J. (2018). High temporal resolution measurement of cognitive and affective processes in psychopathology: What electroencephalography and magnetoencephalography can tell us about mental illness. Biological Psychiatry: Cognitive Neuroscience and Neuroimaging, 3(1), 4-6.
[13] Monllor, P., Cervera-Ferri, A., Lloret, M. A., Esteve, D., Lopez, B., Leon, J. L., & Lloret, A. (2021). Electroencephalography as a non-invasive biomarker of Alzheimer's disease: a forgotten candidate to substitute CSF molecules?. International Journal of Molecular Sciences, 22(19), 10889.
[14] Chuang, K. C., & Lin, Y. P. (2019). Cost-efficient, portable, and custom multi-subject electroencephalogram recording system. IEEE Access, 7, 56760-56769.
[15] Vicchietti, M. L., Ramos, F. M., Betting, L. E., & Campanharo, A. S. (2023). Computational methods of EEG signals analysis for Alzheimer's disease classification. Scientific Reports, 13(1), 8184.
[16] Ando, M., Nobukawa, S., Kikuchi, M., & Takahashi, T. (2021). Identification of electroencephalogram signals in Alzheimer's disease by multifractal and multiscale entropy analysis. Frontiers in Neuroscience, 15, 667614.
[17] Fiscon, G., Weitschek, E., Cialini, A., Felici, G., Bertolazzi, P., De Salvo, S., ... & De Cola, M. C. (2018). Combining EEG signal processing with supervised methods for Alzheimer's patients classification. BMC medical informatics and decision making, 18, 1-10.
[18] Durongbhan, P., Zhao, Y., Chen, L., Zis, P., De Marco, M., Unwin, Z. C., ... & Sarrigiannis, P. G. (2019). A dementia classification framework using frequency and time-frequency features based on EEG signals. IEEE Transactions on Neural Systems and Rehabilitation Engineering, 27(5), 826-835.
[19] Puri, D. V., Kachare, P. H., Sangle, S. B., Kirner, R., Jabbari, A., Al-Shourbaji, I., ... & Alameen, A. (2024). Leadnet: detection of alzheimer's disease using spatiotemporal eeg analysis and low-complexity cnn. IEEE Access.
[20] kumar Ravikanti, D., & Saravanan, S. (2023). EEGAlzheimer'sNet: Development of transformer-based attention long short term memory network for detecting Alzheimer disease using EEG signal. Biomedical Signal Processing and Control, 86, 105318.
[21] Shen, X., Ding, L., Gu, L., Li, X., & Wang, Y. (2024). Diagnosis of Alzheimer's Disease Based on Particle Swarm Optimization Eeg Signal Channel Selection and Gated Recurrent Unit. Available at SSRN 4844658.
[22] Abgeena, A., & Garg, S. (2023). S-LSTM-ATT: a hybrid deep learning approach with optimized features for emotion recognition in electroencephalogram. Health Information Science and Systems, 11(1), 40.